As we proposed, our work evolved from deriving the microphysical basis of rate and state friction [1-3] to applying rate and state friction to nonlinear processes in the shallow subsurface. Our overall philosophy is that obtaining physical understanding of semi-empirical "laws" in rock physics accrues some confidence in extrapolating them to the earth as well as some knowledge of their limitations. We concentrated on damage processes within shallow off-fault environments during the past year. We have shown that 3 observed nonlinear effects are related: (1) The S-wave velocity in the shallow subsurface decreases following strong shaking. The velocity "heals" with the logarithm of time after the event [e.g., 4-8]. (2) Attenuation of strong seismic waves is nonlinear [9-14]. (3) The dynamic stress from strong seismic waves triggers secondary high-frequency events in the shallow subsurface [15-16]. We continue our work on strong ground motions in a productive manner and plan to apply it to extreme ground motions and to near-fault damage. The P.I. has maintained his broad interests in seismology and tectonics.

Off-fault damage. Numerous observations indicate that the S-wave velocity decreases in the aftermath of large nearby events [e.g., 4-8]. Comparison of borehole and surface seismograms indicates that the seismic velocity changes are shallow, <100 m [6,8]. This process shares aspects of damage during frictional sliding predicted by rate and state dependent friction. The S-wave velocity decrease recovers to its pre-quake value with the logarithm of time after the event. The damage from one strong event seems to make the ground more easily damaged by subsequent events [4]. Comparison of the seismograms from weak and intense shaking indicates that attenuation becomes nonlinear at high amplitudes. Recent works include those by *Frankel et al.* [9], *Beresnev* [10], *Hartzell et al.* [11-12], *Bonilla et al.* [13], and *Tsuda et al.* [14]. Comparison of borehole and surface records indicates that the nonlinear response occurs in the shallow subsurface [e.g., 10,13,17,18]. More limited data presented at the 2007 SCEC meeting connect the above nonlinear processes. Strong seismic waves trigger small high-frequency events in the shallow subsurface [15-16]. *Fischer et al.* [16] point out that these events are likely to be both a form of nonlinear attention and a process that damages the shallow subsurface in localized domains.

We began our work on this grant with S-wave velocity changes. An attractive model is that the velocity changes result from dilatancy associated with inelastic shear strain in the shallow subsurface. This process implies work against both friction and lithostatic stress. For purposes of illustration, we model a vertically propagating S-wave with well-known equations. A standing wave represents its reflection from the free surface. The displacement and particle velocity are:

$$u = u_0 \cos(\omega t)\cos(kz); \quad (1) \quad U = -u_0 \omega \sin(\omega t)\cos(kz), \quad (2)$$

where u_0 is the scalar displacement, ω is angular frequency, t is time, k is wave number and z is depth. Dynamic stress causes inelastic deformation and attenuation

$$\tau = -u_0 kG\cos(\omega t)\sin(kz); \quad (3) \qquad \tau_0 = u_0 k^2 Gz. \quad (4)$$

Equation (4) is the Taylor series expression for shallow depths where $kz < 1$. This scalar form yields dimensional approximations for the magnitude of quantities but not their phase. The depth $1/k$ is a natural basis for additional scaling relationships as dynamic stresses are closest to frictional failure criteria $\tau_0 = \mu_0 P = \mu_0 \rho g z$ (where P is confining pressure, μ_0 is the first order coefficient of friction, and g is the acceleration of gravity)

in that region [e.g., 12, p. 1614]. That is, the energy of a reflecting wave is kinetic energy near the free surface that does not cause dissipation and shear-strain energy around the quarter wavelength depth $\pi/2k$. Lithostatic stress continues to increase below the quarter wavelength depth while dynamic stresses are bounded by their value at that depth. The combination of significant shear-strain energy and dynamic stresses near confining pressure imply that nonlinear dissipation should occur around the scale depth if the rock is not fully elastic.

We obtained constraints using the scale depth by considering the balance between the available energy within the incident wave and the energy of damage. Dilated cracks imply work against lithostatic stress as well as some work against friction. The work per volume in both cases scales as strain times lithostatic stress at the scale depth $1/k$,

$$W \approx \frac{\varepsilon \rho g}{k} = \frac{\lambda \Delta f \rho g}{k}, \quad (5)$$

where ε is strain, Δf is the porosity change (volumetric dilatational strain), and $\lambda \geq 1$ is a dimensionless constant that represents the contribution of friction plus dilation.

S-wave velocity changes provide a quantitative way to estimate the porosity change Δf. We use a linear expression to obtain trial dimensional results. The approach applies without loss of generality as a Taylor series approximation over a limited range of porosities when strong motion causes modest damage. Formally,

$$G = \frac{(\gamma - f) G_0}{\gamma}, \quad (6)$$

where the shear modulus extrapolates G_0 at porosity 0 and to 0 at porosity γ. The occurrence of very shallow earthquakes during strong ground motion indicates that damage increases the porosity within highly strained "domains" in the rock that are prone to failure, rather than uniformly. The change in seismic velocity from (6) with respect to porosity is

$$\frac{\partial c}{\partial f} = \frac{\partial}{\partial f}\left(\frac{G}{\rho}\right)^{1/2} = \frac{1}{2\rho^{1/2} G^{1/2}} \frac{\partial G}{\partial f} - \frac{G^{1/2}}{2\rho^{3/2}} \frac{\partial \rho}{\partial f} = -\frac{G_0}{2\rho^{1/2} \gamma G^{1/2}} + \frac{G^{1/2} \rho_0}{2\rho^{3/2}}, \quad (7)$$

where the density of intact rock is ρ_0. As the porosity of rock that fails by cracking is much less than 1, $\gamma << 1$, the second term involving the change in density can be ignored in a dimensional calculation. The S-wave travel time across the easily damaged region of dimensional depth $\sim 1/k$ is simply

$$t_S = \frac{1}{kc} = \frac{1}{\omega}, \quad (8)$$

The change in travel time that occurs over the fixed depth range $1/k$ is

$$\Delta t_S = -\frac{1}{kc^2} \Delta c = -\frac{1}{kc^2}\left[\frac{\partial c}{\partial f}\right] \Delta f = \frac{G_0 \Delta f}{2kc^2 \gamma \rho^{1/2} G^{1/2}} = \frac{\Delta f}{2(\gamma - f)\omega}. \quad (9)$$

where we use (6) to obtain the final equality. That is, the change in travel time is proportional to the product of the original travel time in (8), the porosity change, and a term that relates the change of shear modulus to porosity. Equation (9) has the testable feature that low frequency strong motions cause damage over a great depth range and thus larger travel time anomalies.

For comparison, the strain energy per volume in a propagating seismic wave equals the kinetic energy per volume at every point in space and time,

$$\frac{\tau^2}{2G} = \frac{u_0^2 G k^2}{2}\sin^2(\omega t + kz) = \frac{\rho U^2}{2} = \frac{u_0^2 \rho \omega^2}{2}\sin^2(\omega t + kz) \ , \quad (10)$$

where the equation for seismic velocity $c = \sqrt{G/\rho}$ where ρ is density confirms the final equality [e.g., 1*9*, p. 491]. The kinetic plus strain energy per volume averaged over a wavelength is

$$E = u_0^2 G k^2 / 2 = u_0^2 \rho \omega^2 / 2 . \quad (11)$$

The energy flux per area in the direction of propagation is thus cE. The total energy in a pulse-like arrival is this quantity times the wavelength.

In terms of work per volume in (5), the travel time change is

$$\Delta t_S = \frac{W}{2(\gamma - f)\rho g \lambda c} \ . \quad (12)$$

This quantity is independent of the frequency and equivalently the wavelength of the seismic wave in a half space. However, a low-frequency seismic wave in a real location tends to sample higher velocities at depth than a high frequency wave. Finally, combining (11) and (12) yields the fraction of the wave energy that goes into work to open cracks

$$\frac{W}{E} = \frac{\Delta t_S 2(\gamma - f)\rho g \lambda c}{0.5 U_0^2 \rho} = \frac{\Delta t_S 2(\gamma - f) g \lambda c}{0.5 U_0^2} \quad (13)$$

in terms of measured quantities. More precisely, the energy of a pulse-like arrival is distributed integrated its wavelength is $2\pi E/k$ while the energy per area to open cracks within a vertical column scales as a W/k. We do not make the distinction in these dimensional results for simplicity.

Finally, the tendency of a material to fail in friction or dilation depends on the ratio of dynamic stresses to lithostatic stresses. This Coulomb ratio above the scale depth is

$$\frac{\tau_0 k}{\rho g} = \frac{u_0 G k^2}{\rho g} = \frac{u_0 \rho c^2 k^2}{\rho g} = \frac{u_0 \omega^2}{g} = \frac{A_0}{g}, \quad (14)$$

which is the measured ratio of particle acceleration to gravity and independent of material properties. This mechanical definition of strong motion in (14) is equivalent to the conventional definition that sustained accelerations are on the order of that of gravity. This useful relationship is entrenched in work on the nonlinear attenuation of seismic waves. For example, *Beresnev* [10] compiled amplification ratio as a function of peak ground acceleration.

We provide a generic example applicable to the 2004 Parkfield earthquake [20]. The dominant angular frequency ω is 10 s^{-1} and the maximum velocity is 0.5 m s^{-1}. The maximum displacement is 0.05 m. The S-wave velocity in the upper 30 m is ~300 m s^{-1} at many sites. The scale depth $1/k$ is 30 m, implying that VS30 in seismic station tables is an appropriate estimate of seismic velocity in the region where damage is likely. *Rubenstein and Beroza* [6] observed a typical S-wave travel time change of 0.007 s. We obtain the porosity from (6) with reasonable parameters: the failure porosity be $\gamma = 0.24$, the intact shear modulus be G_0= 20 GPa, and the density ρ = 2000 kg m^{-3}. This yields that the porosity is 0.24-0.00216 = 0.2234. The velocity change ~7% implies a porosity

increase of 0.0003. This would produce and uplift scaling to $\Delta f / k$ of 0.009 m, which would be marginally observable. The work per volume from (5) letting $\lambda = 1$ is 180 J m^2. The energy per volume in the wave from (5) is 250 J m^2. The ratio in (13) is 0.72. The diminution of the upcoming energy is 0.72/(1 + 0.72) = 0.56. We note that this quantity as a stable measure of nonlinear attenuation.

Our work provides key physical inferences on the physical causes of attenuation: (1) Our computed Parkfield attenuation is significant. The parameter λ cannot have its value ~25 for laboratory sliding friction [3. 21] since this would imply attenuation of more than the available seismic energy. This result implies kinematic dilatancy at small strains from rolling irregular grains and asperities sliding over one another. (2) With additional mathematics, the computed macroscopic porosity change is an average of undamaged rock and a few damaged domains as expected from the occurrence of small shallow earthquakes [15.16] during strong shaking. The logarithmic dependence of seismic velocity with time after the strong shaking involves healing of the damaged domains and is incompatible with uniformal distributed damage. (3) With additional calculations, crack opening can attenuate significant energy in hard rocks without measurably changing the seismic velocity. (4) With more calculation, damage occurs over a range of dynamic stress as in engineering treatments of nonlinear attenuation [e.g., 12,22], implying the ground has variable (probably fractal) pre-stress [23] and strength.

Publications. We continue to prepare a paper [24] that presents to the energy balance discussed above and examines more sophisticated ways to relate S-wave velocity to porosity and to starting frictional strength. We have found that the *Linker and Dieterich* [25] relationship allows one to extrapolate experimental frictional strength toward low confining pressures (Figure 1). One goal is to calibrate the maximum strength of the shallow subsurface and thus obtain limits on extreme ground motions. Significant nonlinear attention occurs well before the maximum strength. That is, observation of modest nonlinear effects (including attenuation, S-wave velocity changes, and small shallow earthquakes) during moderate ground motion indicate that somewhat stronger upcoming waves would be strongly attenuated.

Our second paper [26] that relates to extreme ground motion is in press. For example, *Shakal et al.* [27] discuss brief pulses of >2 g acceleration during the 2004 Parkfield event. We utilize the observation of small earthquakes in the shallow subsurface during strong shaking [15,16]. Larger events would cause brief extreme ~2 g ground accelerations (Figure 2). They require that dynamic stress drives faulting on ruptures with dimensions comparable to the depth and that the stress drop is nearly total. Such events leave residual stresses with the opposite sense of the dynamic stress after shaking has ceased. This process shares a feature with other nonlinear mechanisms with pulse-like upcoming arrivals; the peak dynamic stress near the quarter-wavelength depth occurs in the later part of the strong motion when the reflected first part of the pulse interacts with the upcoming part of the pulse with the opposite polarity. This hypothesis implies that brief extreme acceleration pulses are a form of nonlinear attenuation that converts the lower frequency energy of the incoming pulse partly into higher frequency energy, rather than harbingers of sustained extreme accelerations produced on the main fault plane.

We include a second nonlinear mechanism is this paper that applies to rocks with compliant fractures and stiff intact domains. The sandstones at Parkfield are an example. The rock mass is compliant and has a low ~300 m/s S-wave velocity at small strains. At

large strains asperities in the cracks lock and the rock mass becomes stiff. We found that this mechanism does produce extreme accelerations. Our work is useful in that it constrains the amount of stiffening needed to produce significant effects.

We continue to apply rate and state friction to examine nonlinear effects in the shallow subsurface and near fault damage. With regard to the shallow subsurface, the logarithmic healing of S-wave velocity is the strongest indication that time-dependent Coulomb friction is applicable. In addition, nonlinear effects become evident when dynamic stresses become a fraction of lithostatic stress. Our approach (as already noted) yields the traditional result for site effects: nonlinear attenuation increases from minor to significant with an increase of strong ground motion by a factor of a few. There are two useful ways to parameterize the limit to extreme dynamic stress: (1) There is a dynamic stress where attenuation becomes strong enough that further increases in the amplitude of the upcoming wave do not greatly augment the shaking at the surface. (2) There is a higher dynamic stress that would pulverize the rock (Figure 1). We have reasonable formalism for the latter [28-30] and will concentrate on obtaining up limits to extreme ground motion from observable quantities including S-wave velocity and well collapse.

Surface waves and reverberating waves in sedimentary basins imply energy that repeatedly passes through the shallow subsurface. A site approach to nonlinear attenuation is thus inapplicable. These waves imply modest ratios of dynamic stress to lithostatic stress. Still much of the seismic energy is subject to nonlinear attenuation at any given time. We continue examine simple ways to constrain and parameterize this effect.

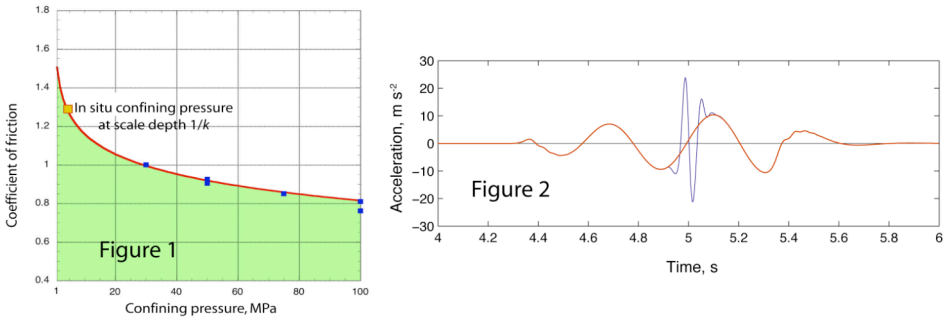

Figure 1: The starting coefficient of friction for the McDarley Dale sandstone as a function of confining pressure [31-32]. The *Linker and Dieterich* relationship [25] allows explanation to lower confining pressure. The coefficient of friction near the scale depth is relevant to the transmission of extreme seismic waves and approximately maximum sustainable acceleration. The starting coefficient of friction of more cracked and lower VS rock lies in the shaded region below the curve.

Figure 2. Computed acceleration for a secondary earthquake driven by dynamic stress. The calculation is 2-D plane strain using the code from the work of *Andrews* [33]. The incident arrival is a vertically propagating S-wave The secondary fault is 30 m wide and 30 meters deep. The smooth curve is the linear response to the assumed incident pulse (obtained by smoothing from the 2004 arrival at station FZ 16 Parkfield [27]). Extreme acceleration from the secondary rupture arrives around 5 s. The curves are otherwise identical.

[1] Sleep, N. H. (2005) Physical basis of evolution laws for rate and state friction, *Geochem. Geophys. Geosyst.*, *6*, Q11008, doi:10.1029/2005GC000991. *SCEC contribution number 896.*

[2] Sleep, N. H. (2006) Real contacts and evolution laws for rate and state friction, *Geochem. Geophys. Geosyst.*, *7*, Q08012, doi:10.1029/2005GC001187. *SCEC contribution number 991.*

[3] Sleep, N. H. (2006) Frictional dilatancy, *Geochem. Geophys. Geosyst.*, *7*, Q10008, doi:10.1029/2006GC001374. *SCEC contribution number 1030.*

[4] Rubinstein, J. L., and G. C. Beroza (2004a) Nonlinear strong ground motion in the M_L 5.4 Chattenden earthquake: Evidence that preexisting damage increases susceptibility to further damage, *Geophys. Res. Lett., 31*, L23614, doi:10.1029/2004GL021357.

[5] Rubinstein, J. L., and G. C. Beroza (2004b) Evidence for widespread nonlinear strong motion in the M_W 6.9 Loma Prieta Earthquake, *Bull. Seismol. Soc. Am., 94*, 1595-1608.

[6] Rubinstein, J. L., and G. C. Beroza (2005) Depth constraints on nonlinear strong ground motion from the 2004 Parkfield earthquake, *Geophys. Res. Lett., 32*, L14313, doi:10.1029/2005GL023189.

[8] Sawazaki, K., H. Sato, H. Nakahara, and T. Mishimura (2006) Temporal change in site response caused by earthquake strong motion as revealed from coda spectral ratio measurement, *Geophys. Res. Lett, 33*, L21303, doi: 10.1029/2006GL027938.

[9] Frankel, A. D., D. L. Carver, and R. A. Williams (2002) Nonlinear and linear site response and basin effects in Seattle for the M 6.8 Nisqually, Washington, earthquake, *Bull. Seism. Soc. Am.*, *92***,** 2090–2109.

[10] Beresnev, I. A. (2002) Nonlinearity at California generic soil sites from modeling recent strong-motion data, *Bull. Seismol. Soc. A., 92*, 863-870.

[11] Hartzell, S., A. Leeds, A. Frankel, R. A. Williams, J. Odum, W. Stephenson, and W. Silva (2002) Simulation of broadband ground motion including nonlinear soli effects for a magnitude 6.5 earthquake on the Seattle Fault, Seattle, Washington, *Bull. Seismol. Soc. Am., 92*, 831-853.

[12] Hartzell, S., L. F. Bonilla, and R. A. Williams (2004) Prediction of nonlinear soil effects, *Bull. Seismol. Soc. Am., 96*, 1609-1629.

[13] Bonilla, L. F., R. J. Archuletta, and D. Lavallée (2005) Hysteretic and dilatant behavior of cohesionless soils and their effects on nonlinear site response: Field data observations and modeling, *Bull. Seismol. Soc. A., 95*, 2373-2395.

[14] Tsuda, K., J. Steidl, R. Archuleta, and D. Assimaki (2006a) Site-response estimation for the 2003 Miyagi-Oki earthquake sequence consider nonlinear site response, *Bull. Seismol. Soc. Am., 96*, 1474-1482.

[15] Fischer, A. D., C. G. Sammis, Y. Chen, and T.-L. Teng (2008) Dynamic triggering by strong motion P- and S-waves: Evidence from 1999 Chi-Chi, Taiwan Earthquake, Bull. Seismol. Soc. Am., in press.

[16] Fischer, A. D., Z. Peng, and C. G. Sammis, (2008) Dynamic triggering of high-frequency bursts by strong motions during the 2004 Parkfield earthquake sequence, *Geophys. Res. Lett.*

[17] Tsuda, K., R. J. Archulete, and K. Koketsu (2006b) Quantifying the spatial distribution of site response by use of the Yokohama high-density strong-motion network, *Bull. Seismol. Soc. Am., 96*, 926-942.

[18] Lee, C.-P., Y.-B. Tsai, and K.-L. Wen (2006) Analysis of nonlinear site response using the LSST downhole accelerometer array data, *Soil Dynamics Earthquake Engineering*, 26, 435-460.

[19] Timoshenko, S. P., and J. N. Goodier, (1970) *Theory of Elasticity*, McGraw-Hill New York, 567 pp.

[20] Shakal, A. F., H. R. Haddadi, V. Graizer, K. Lin, and M. Huang (2006a) Some key features of the strong-motion data from the **M** 6.0 Parkfield, California, earthquake of 28 September 2004, *Bull. Seismol. Soc. Am., 96*, S90-S118.

[21] Segall, P., and J.R. Rice (1995) Dilatancy, compaction, and slip-instability of a fluid-penetrated fault, *J. Geophys. Res.*, *100*(B11) , 22,155-22,171.

[22] Kramer, S. L. (1996) Geotechnical Earthquake Engineering, Prentice Hall, Upper Saddle River, N.J., 653 pp.

[23] Marsan. D. (2005) The role of small earthquakes in redistributing crustal elastic stress. *Geophys. J. Int., 163*, 141-151.

[24] Sleep, N. H., and P. Hagin (in prep) Nonlinear attenuation and rock damage during strong seismic ground motions. *Geochem. Geophys. Geosyst.*

[25] Linker, M. F., and J. H. Dieterich (1992) Effects of variable normal traction on rock friction: Observations and constitutive equations, *J. Geophys. Res.*, *97*(B4), 4923-4940.

[26] Sleep, N. H. and S. Ma (in press) Production of brief extreme ground acceleration pulses by nonlinear mechanisms in the shallow subsurface**,** *Geochem. Geophys. Geosyst.*

[27] Shakal, A. F., H. R. Haddadi, and M. J. Huang (2006b) Note on the very-high-acceleration Fault Zone 16 record from the 2004 Parkfield earthquake, *Bull. Seismol. Soc. Am., 96*, S119-S128.

[28] Lockner, D. A., (1995) Rock failure, in *Rock Physics and Phase Relations: A Handbook of Physical Constants*, *AGU Ref. Shelf Ser.*, v. *3*, p. 127-147

[29] Sleep, N. H., (1999) Rate- and state-dependent friction of intact rock and gouge, *J. Geophys. Res.*, *104*, 17,847-17,855.

[30] Hagin, P., N. H. Sleep, and M. D. Zoback (2007) Application of rate-and-state friction laws to creep compaction of unconsolidated sand under hydrostatic loading conditions, *J. Geophys. Res.*, *112*, B05420, doi:10.1029/2006JB004286.